Providence College
DigitalCommons@Providence

Chemistry Department Student Papers   Chemistry

2016

Mutation of Surface Histidines in *Haemophilus influenzae* Carbonic Anhydrase to Enable Purification by Metal Affinity Chromatography

Shelby E. Scola
Providence College

Kathleen Cornely
Providence College

Follow this and additional works at: http://digitalcommons.providence.edu/chemistry_students

Part of the Chemistry Commons

Mutation of Surface Histidines in *Haemophilus influenzae* Carbonic Anhydrase to Enable Purification by Metal Affinity Chromatography

Shelby E. Scola and Dr. Kathleen Cornely

From the Department of Chemistry and Biochemistry, Providence College, Providence, Rhode Island 02918

H. influenzae carbonic anhydrase (HICA) is a β-carbonic anhydrase that is important to the survival of the human respiratory tract pathogen *H. influenzae*. Although HICA shares a high degree of structural similarity with *E. coli* carbonic anhydrase (ECCA), HICA lacks ECCA's nickel-binding capabilities. However, previous research suggests that the engineering of histidine clusters on HICA through the mutation of surface residues enables HICA to gain nickel-binding ability similar to that of ECCA. Here we present the production and analysis of a K129 L133 HICA double mutant. Using PyMOL to visualize the mutant, it was determined that the mutated histidines form a cluster of four histidines which are all located between approximately 3.7 to 6.7 Å from each other. The mutant plasmid was constructed using site-directed mutagenesis via megaprimer PCR, and then overexpressed in *E. coli* to obtain a protein lysate with a protein concentration of 16.23 ± 0.06 mg/mL. The ability of the mutant HICA protein to bind to nickel was analyzed using Ni-NTA chromatography, followed by SDS-PAGE analysis of the chromatography fractions. The results of the SDS-PAGE analysis suggest that the mutant HICA protein bound weakly to the nickel column, requiring 25 mM imidazole to elute.

Carbonic anhydrases are zinc metalloenzymes that catalyze the reversible interconversion of CO_2 and bicarbonate:

$$CO_2 + H_2O \rightleftharpoons HCO_3^- + H^+$$
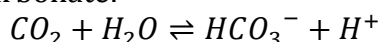
Haemophilus influenzae carbonic anhydrase (HICA) is a member of the β-form of carbonic anhydrases, a class of enzymes found in bacteria, yeast, and plant chloroplasts (1). HICA is essential for the survival of nontypeable (unencapsulated) strains of *H. influenzae* bacteria in ambient air and intracellular survival in host cells. These bacterial strains are one of the leading causes of noninvasive mucosal infections, such as otitis media, sinusitis, and conjunctivitis (2). Therefore, HICA could be a potential antibiotic target in the treatment of these infections. However, the potential to carry out further research on HICA hinges on the ability to purify it in large quantities.

Purification of HICA and other proteins is commonly achieved by metal affinity chromatography after a histidine tag has been engineered onto the N-terminus or C-terminus of the polypeptide chain. Some advantages of this method are its ability to purify proteins in one step and the ease of imidazole elution. However, drawbacks include potential interference of tags with quaternary structure or the introduction of random coiling that could interfere with downstream techniques. If the tag is close to the active site, it could change the conformation of the protein, resulting in proteins that have lost their function. Sometimes this can be fixed by moving the tag to the opposite terminus, but this does not always prove effective (1).

Since some *E. coli* proteins have been discovered that exhibit endogenous nickel affinity, it is possible that instead of engineering a terminal histidine tag, metal affinity could be engineered on the surface of a protein. Since four of the six ligand positions on Ni^{2+} ions are usually occupied by other ligands, theoretically only two histidines may be necessary for nickel binding. Based on known inorganic structures, the optimal distance between these two histidines is expected to be between 4 and 7 Å apart (1). Although histidine tags are usually engineered with six adjacent histidines at the terminus, proteins could be engineered to have histidine clusters to mimic those of proteins with endogenous nickel affinity. A better understanding of the parameters of histidine location on the surface of proteins required for metal-affinity chromatography would provide a broadly applicable technique for protein purification and eliminate the need to use histidine tags. To begin defining these parameters, proteins with endogenous metal affinity must first be examined.

One such protein that exhibits endogenous metal affinity and is closely related to HICA is *E. coli* carbonic anhydrase (ECCA), which has been shown to bind to so tightly to Ni^{2+} columns that 250 to 300 mM imidazole is needed to elute it (1). Like other β-carbonic anhydrases, ECCA's quaternary structure is a dimer of dimers. The tetramerization interface between dimers is partially solvent exposed and contains two symmetry-related clusters of histidines. Each cluster includes six histidines from two chains (His72, His122, and His160 from one chain; His720, His1220, and His1600 from the other chain). Within the same chain, the histidines are between 5 and 7 Å apart, while the interchain distances are closer to 3.5 and 4.5 Å. These side chains could be within the sphere of rotation necessary to optimize nickel coordination since nickel(II)–histidine coordination distances have been observed in protein structures at 1.8 to 2.4 Å (1).

Recognizing that HICA, while unable to bind to Ni^{2+}, does share 38% identity, quaternary structure, and activity profile similar to ECCA, and only partially conserves the cluster of histidines in the tetramerization interface (His72, His122, and Arg160), Hoffman explored the possibility of mutating HICA's Arg160 residue to histidine to recreate ECCA's metal affinity. While wildtype HICA does not bind to the nickel column, the Arg160 mutant was shown to elute with 190 mM imidazole, while ECCA elutes at 278 mM imidazole. Furthermore they reported that while optimizing Arg160His HICA's purification to minimize secondary retention during the binding and wash steps meant that the protein variant eluted earlier in the gradient, the HICA mutant similarly achieved greater than 90% purity. In addition, the surface mutations did not influence the overall structure or function of the HICA protein, since steady-state kinetic activity and oligomerization state were similar to that of wildtype HICA (1).

Using their work as a model, we wanted to explore the possibility of increasing the metal affinity of HICA by mutating other solvent-exposed residues besides Arg160. We chose to engineer a double mutant in which both Lys129 and Leu133 residues were mutated to histidine, as these residues were present on the surface of the HICA protein and were located in close proximity (within 4.4 to 6.4 Å) to two other histidines. The goal was for these four histidines to be close enough to form a cluster to optimize nickel coordination. Here we report the successful generation of a K129 L133 mutant HICA protein, and its ability to bind weakly to the nickel columns, requiring 25 mM imidazole to elute.

EXPERIMENTAL PROCEDURES

    Cultures – DH5α *E. coli* cells transformed with pHICA were obtained as frozen stock from the Hoffman laboratory. Cells were taken from frozen stock and inoculated in LB medium containing 1% tryptone, 0.5% yeast extract, 1% NaCl, and 100 µg/mL ampicillin. Cultures were incubated in a roller drum for 23 hours at 37°C.

    Plasmid miniprep – A plasmid miniprep for the pHICA plasmid was performed using a Zymo Zyppy Plasmid Miniprep Kit from Zymo Research. Kit instructions were followed with the only exception being that the samples were incubated with Zyppy Elution Buffer for 20 min instead of 1 min. Plasmid DNA concentrations were determined via NanoDrop 1000 Spectrophotometer (ThermoScientific) to be 95.7 ng/µL.

    Site-Directed Mutagenesis (3)– In order to amplify the mutation of interest to produce a megaprimer, a PCR mixture containing 3.83 ng/µL pHICA plasmid template, 1 pmol/µL forward primer containing mutations (5'-GGTTT<u>C</u>A<u>T</u>CACGGTCATC<u>A</u>TCTCG-3'), 1 pmol/µL reverse primer Phi2X (5'-AGCTTGCATGCCTGCCTGCAGTTATTATG-3'), 0.2 mM dNTP mix, Phusion HF Buffer, and 0.05 units/µL Phusion High-Fidelity DNA polymerase was made. This sample underwent touchdown PCR (4) with the following protocol: one initial cycle at 95 °C for 2 min; 40 cycles of 95 °C for 30 sec, 65 °C for 30 sec (temperature lowered 0.5 °C per cycle), and 72 °C for 30 sec; one cycle at 72 °C for 10 min; then hold at 4 °C. The sample was run on a 1% agarose gel containing TAE (0.04 M Tris, 1 mM EDTA, 0.02 M glacial acid). In order to visualize the bands, 0.001 % SYBR Safe DNA gel stain from Life Technologies was used. Bands were excised and purified using the Zymoclean Gel DNA Recovery Kit from Zymo Research. Instructions were followed with the exception that incubation was performed using pre-warmed (48 °C) elution buffer and samples were incubated for 7 min.

    In order to amplify the entire HICA gene containing the mutation, a PCR sample containing 3.83 ng/µL pHICA template, 1 pmol/µL PhiQC primer (5'-CACTGCATAATTCGTGTCGCTCAAGG-3'), a third of the megaprimer sample obtained from the previous round of PCR, 0.2 mM dNTP mix, Phusion HF Buffer, and 0.05 units/µL Phusion High-Fidelity DNA polymerase was made. This sample underwent classic PCR, with an initial cycle at 95°C for 2 min; 30 cycles of 95°C for 30 sec, 55°C for 30 sec, and 72°C for 1 min; an extension cycle of 72°C for 10 min; and then a final cycle held at 4°C. The sample was run on a 1% agarose gel containing TAE (0.04 M Tris, 1 mM EDTA, 0.02 M glacial acid). In order to visualize the bands, 0.001 % SYBR Safe DNA gel stain from Life Technologies was used. Bands were excised and purified using the Zymoclean Gel DNA Recovery Kit from Zymo Research. Instructions were followed with the exception that incubation was performed using pre-warmed (48 °C) elution buffer and samples were incubated for 10 min.

    In order to amplify the entire pHICA plasmid containing the mutation, a PCR sample containing 3.83 ng/µL pHICA template, a third of the megaprimer sample obtained from the previous round of PCR, 0.2 mM dNTPs, Phusion HF Buffer, and 0.05 units/µL Phusion High-Fidelity DNA polymerase. This sample underwent classic PCR, with an initial cycle at 95°C for 2 min; 30 cycles of 95°C for 1 min, 60°C for 1 min, and 72°C for 5 min; an extension cycle of 72°C for 10 min; and then a final cycle held at 4°C. The sample was run on a 0.8% agarose gel containing TAE (0.04 M Tris, 1 mM EDTA, 0.02 M glacial acid). In order to visualize the bands, 0.001% SYBR Safe DNA gel stain from Life Technologies was used.

Transformation of mutant pHICA into E. coli cells – In order to obtain a higher quantity of mutant pHICA plasmid, the plasmid was transformed into *E. coli* cells. First, PCR samples were treated with 10 units of Dpn1 enzyme in order to digest the parent plasmid DNA. Samples were then incubated for approximately 2.5 hours at 37°C. Following incubation, 2.5 µL of the Dpn1-treated sample was added to 50 µL of DH5α competent *E. coli* cells from Zymo Research Mix and Go *E. coli* Transformation Kit and Buffer Set. Following a 30 min incubation on ice, samples were plated on pre-warmed LB + amp plates (100 µg/mL ampicillin) and incubated overnight at 37°C. A transformant colony was inoculated in LB + amp medium and incubated overnight at 37°C.

Sequencing – To prepare a sample for sequencing, the liquid culture was centrifuged and the pellet was resuspended in 1 mL of LB + amp medium. A plasmid miniprep was then performed on the sample using a Zymo Zyppy Plasmid Miniprep Kit. Kit instructions were followed with the only exception being that the samples were incubated with pre-warmed (48 °C) Zyppy Elution Buffer for 30 min instead of 1 min. Plasmid DNA concentrations were determined via NanoDrop 1000 Spectrophotometer to be 29.0 ng/µL. The sample sent for sequencing contained 21.8 ng/µL plasmid DNA, 1.5 µM PRRXseqforward primer (5'-GGCTCGTATAATGTGTGGAATTG-3'), and TE buffer (10 mM Tris, 1 mM EDTA) to obtain a total volume of 20 µL. The plasmid sample was shipped to the MGH Core Facility for sequencing.

Transformation of mutant pHICA plasmid into autolysis cells – In preparation for transformation, DH5α *E. coli* cells containing the mutant plasmid were inoculated in 5 mL LB + amp medium, incubated overnight at 37 °C, and then underwent a plasmid miniprep using a Zymo Zyppy Plasmid Miniprep Kit. Kit instructions were followed with the only exception being that the samples were incubated with pre-warmed (48 °C) Zyppy Elution Buffer for 30 min instead of 1 min. Mutant plasmid DNA concentrations were determined via NanoDrop 1000 Spectrophotometer to be 75.0 ng/µL. A transformation mixture containing 3.57 ng/µL mutant plasmid and 50 µL of XJb Autolysis *E. coli* cells from Zymo Research was incubated on ice for 15 min, then plated on pre-warmed (37 °C) LB + amp plates. The plates were incubated overnight at 37 °C.

Production scale overexpression of folded mutant HICA protein – LB + amp liquid cultures of XJb *E. coli* transformants with the mutant plasmid were pelleted at 8000 × g for 5 min, then the pellets were resuspended in 10 mL LB + amp medium. These cells were inoculated in medium containing 900 mL TB nutrient (1.33% w/v tryptone, 2.67% w/v yeast extract, 0.44% glycerol), 100 mL TB buffer (0.89 M phosphate, pH 8), ampicillin, and 3 mM arabinose, and incubated for approximately 3 hours. Then 0.2 mM IPTG was added to induce expression of the mutant protein. Cells were incubated overnight with shaking at 37°C. Cells were harvested by centrifugation at 8000 × g for 10 min. The resulting wet cell pellet weighed 10.488 g. The pellet was frozen and then subsequently thawed to lyse cells.

Cell lysis – Cells were resuspended in ~3 mL extraction buffer (20 mM Tris, 200 mM NaCl, pH 8) per gram of cell pellet. Half of a Pierce protease inhibitor mini-tablet from Thermo Scientific was added to the mixture, and the mixture was incubated at 37 °C with vigorous shaking until homogenous. In order to reduce clumping, 16 units of DNAse I from New England BioLabs were added to the sample. Following incubation, the mixture was centrifuged at 35,000 × g for 30 min. The supernatant was then centrifuged for an additional 15 min at 35,000 × g.

BCA assay – A BCA assay (5) was performed using the Pierce BCA Protein Assay Kit from Thermo Scientific to determine the protein concentration of the lysate containing soluble mutant HICA proteins. Kit instructions were followed with the only exception being that the BSA standards were purchased rather than prepared. The standards used were a set of BSA standards (concentrations ranging from 125 µg/mL to 2000 µg/mL) from Thermo Scientific. In addition, the sample of unknown concentration (the lysate of soluble mutant HICA proteins) was diluted $1/_{20}$ so that the concentration would fall within the range of the standards. Absorbance values at 562nm were obtained using a Cary 50.

Ni-NTA Chromatography (6) – To prepare an equilibrated matrix, 2 mL of Ni-NTA slurry (1 mL bed volume) from Qiagen was centrifuged at 2500 rpm, the supernatant was removed, 4 mL of lysis buffer (20 mM Tris, 200 mM NaCl, pH = 8) was added, the mixture was inverted to mix, centrifuged again at 2500 rpm, and the supernatant was removed. To this equilibrated matrix, 8 mL of protein lysate (thawed on ice) and 10 mM imidazole were added, and the mixture was incubated for 60 min with shaking at 4°C. Following incubation, the lysate-Ni-NTA mixture was loaded into a column and the flow-through (the first 8 column volumes) was collected. The next 15 column volumes were washed with 25 mM imidazole, then 5 column volumes were washed with 50 mM imidazole, 5 column volumes were washed with 75 mM imidazole, 5 column volumes were washed with 100 mM imidazole, 4 column volumes were eluted with 250 mM imidazole, 4 column volumes were eluted with 500 mM imidazole, and finally 3 column volumes were eluted with 2 M imidazole. These fractions were collected for SDS-PAGE analysis.

SDS-PAGE analysis – For SDS-PAGE analysis of the fractions from the Ni-NTA chromatography, Laemmli procedure (7) was followed with the exception that a 12.5% separating gel was prepared containing lower Tris buffer (1.5 M Tris, 0.4% SDS, pH = 8), 12.5% acrylamide/0.33% bis-acrylamide, 0.03% ammonium persulfate, and 0.025% TEMED (N,N,N',N'-tetramethylethylenediamine). The stacking gel prepared contained upper Tris buffer (0.5 M Tris, 0.4% SDS, pH = 8), 3% acrylamide/0.08% bis-acrylamide, 0.03% ammonium persulfate, and 0.1% TEMED. The samples contained Laemmli sample buffer (0.063 M Tris, 10% glycerol, 2 mM DTT, 2.3% SDS, 1% β-mercaptoethanol, pH = 6.8). Samples were incubated at 100 °C for 3 min. Then the gel was run for approximately 5 hours with a Tris/glycine reservoir buffer (0.025 M Tris, 0.192 M glycine, 0.1% SDS, pH = 8.3) at 55 mamps for the separating gel and 30 for the stacking gel. Following electrophoresis, the gel was stained overnight with 0.025% Coomassie Blue R-250 staining solution containing 40% MeOH and 7% HAc, and subsequently destained with a destaining solution containing 3% glycerol, 10% HAc, and 40% MeOH. The destaining solution was changed twice over a 3 day period. The gel was dried in a gel dryer for 2 hours at 80 °C and then 30 min at room temperature.

RESULTS

PyMOL analysis – Analysis of the HICA protein in PyMOL revealed that residues K129 and L133 were viable for mutation to His because these residues were both within 4.4 to 6.4 Å of pre-existing His residues (Fig. 1A). If these residues were to be mutated to His, the estimated distances between the mutated His residues and the pre-existing His residues would be between 3.7 to 6.7 Å (Fig. 1B), so these residues could potentially form a His cluster that could bind to the nickel column.

Site-directed mutagenesis – In order to amplify a region of the HICA gene containing the K129 and L133 mutations, a PCR reaction was performed and the resulting product was run on a gel to verify the length of the DNA fragment produced. The calculated size of the expected DNA fragment was 342 bp, and the PCR product appeared between 300 and 400 bp on the DNA gel (Fig. 2A).

Using this PCR product that contained the K129 and L133 mutations as a megaprimer, another PCR reaction was performed in order to amplify the entire HICA gene containing the K129 and L133 mutations. The result of this second PCR reaction was run on gel to verify that PCR produced the expected product. The calculated size of the expected DNA fragment containing the entire HICA gene was 883 bp, and the PCR product appeared around 1,000 bp on the DNA gel (Fig. 2B).

Using this PCR product of the entire HICA gene containing the K129 and L133 mutations as a megaprimer, another PCR reaction was performed in order to amplify the entire pHICA plasmid containing the K129 and L133 mutations. The result of this third PCR reaction was run on a gel to verify that PCR produced the expected product. The calculated size of the expected DNA fragment was approximately 5 kb, and while the PCR sample formed some smeared bands on the gel, there was a band around 6 kb that was assumed to be the mutant pHICA plasmid (Fig. 2C). Sequencing of this plasmid confirmed that the K129 and L133 mutations were present.

BCA Assay – As shown in Fig. 3, a standard curve was created by plotting absorbance at 280nm vs. protein concentration of the BSA standards. From the linear regression performed on the standard curve, the amount of protein in the cell lysate from the lysed XJb *E. coli* cells could be quantified. The concentration of protein in the cell lysate was determined to be 16.23 ± 0.06 mg/mL. However, this number represents the total protein concentration, not just the concentration of mutant HICA protein.

Ni-NTA Chromatography and SDS-PAGE analysis – Since the mutant protein has two extra His residues, it is expected to bind more tightly to a nickel column than the wildtype HICA protein, which is not retained by nickel columns (1). Ni-NTA chromatography was therefore carried out in order to assess the mutant HICA protein's affinity for nickel. Though the elution profile shows a spike in absorbance at 280nm when 100 mM and 250 mM imidazole solutions were applied to the column (Fig. 4), an SDS-PAGE analysis was necessary to determine whether or not these fractions contained the mutant HICA protein. The mutant protein was expected to be about 26 kDa. Bright bands of around size were present in the SDS-PAGE gel in lanes that contained the cell extract, flow-through, and wash 1, and very faint bands of this size appeared in the other lanes as well (Fig. 5). These faint bands were deemed insignificant, as most of the protein eluted in the preceding lanes. Since wash 1 was a 25 mM imidazole wash, it was concluded that the mutant HICA protein only required up to 25 mM imidazole to elute.
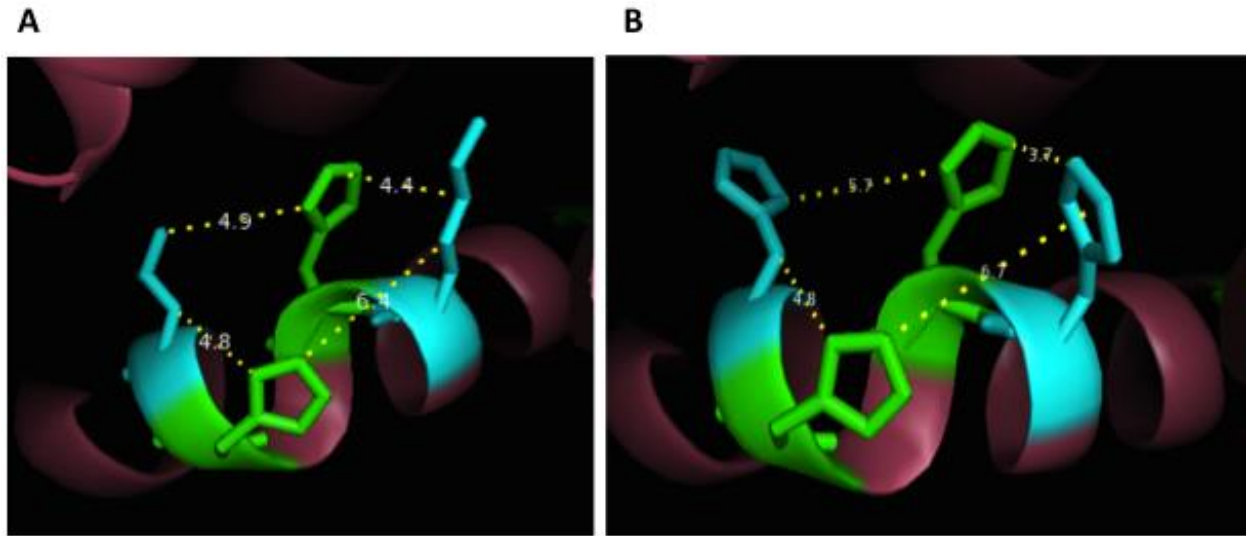
FIGURE 1. **Pymol images of mutated amino acids K129 and L133.** *A*, amino acid side chains before K129 and L133 residues mutated. *B*, amino acid side chains after residues mutated to His. Green-colored histidines are pre-existing proximal histidines, cyan-colored amino acids are the residues of interest for mutation, and yellow dotted lines indicate distances (in Å) between various residues.
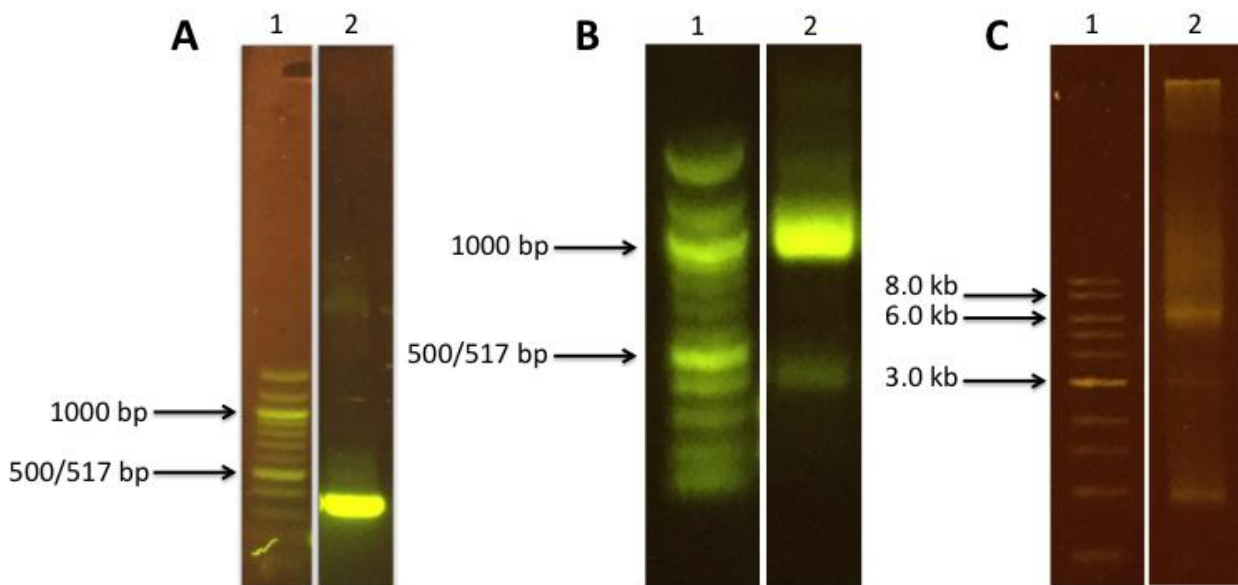

FIGURE 2. **Gels for length verification for K129 L133 mutation region, HICA gene, and pHICA plasmid.** *A*, PCR products from the amplification of the K129 L133 mutation region. *B*, PCR products from the amplification of the HICA gene. *C*, PCR products from the amplification of the pHICA plasmid.
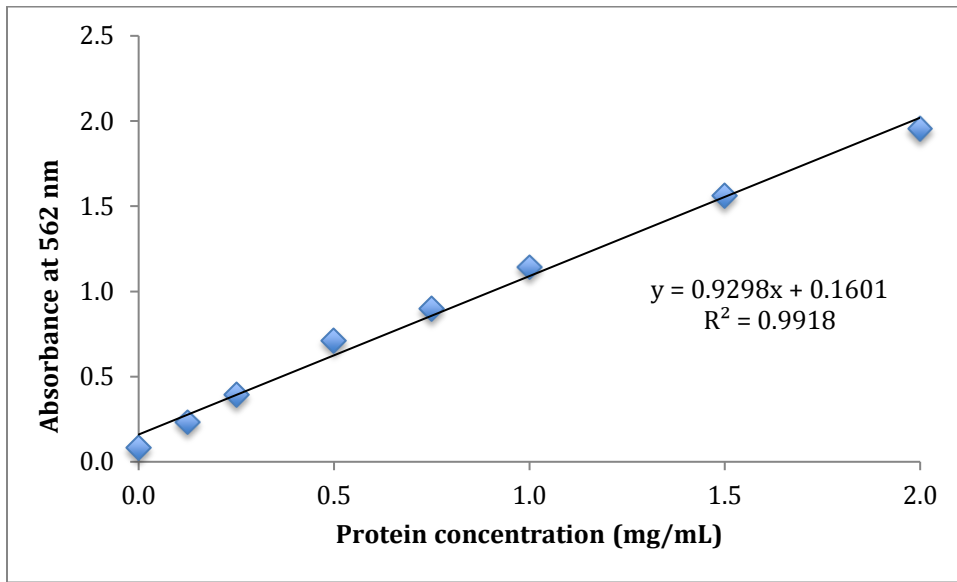
FIGURE 3. **Standard curve for BCA assay.** Points represent data from the BSA standards. The linear regression equation is Abs = 0.9298(conc.) + 0.1601, with R_2 = 0.99183.
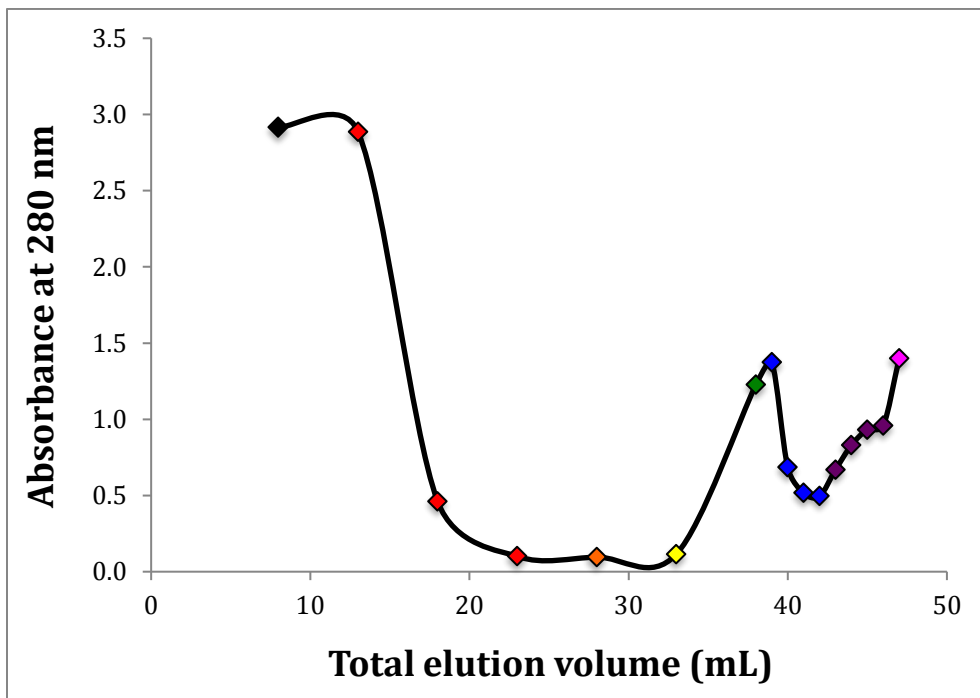

FIGURE 4. **Ni-NTA chromatography elution profile.** The protein lysate sample containing the soluble mutant plasmid was passed through a Ni-NTA column (1 column volume = 1 mL). The first 8 column volumes were flow-through and the following column volumes were washed with various concentrations of imidazole (see Table 1).

Table 1
Key for Ni-NTA chromatography elution profile (Fig. 4).

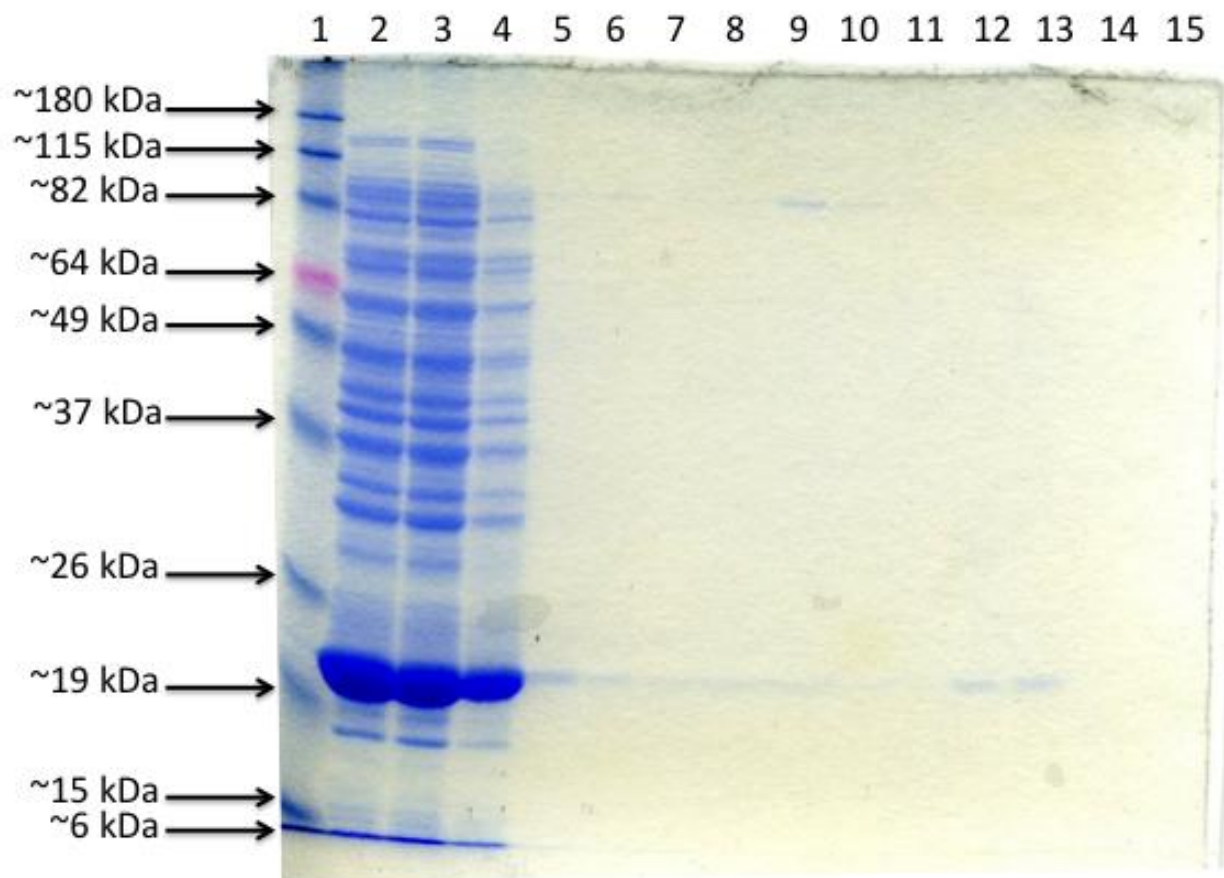| color	column vol	imidazole conc. (mM)
black	1-8	0
red	9-23	25
orange	24-28	50
yellow	29-33	75
green	34-38	100
blue	39-42	250
purple	43-46	500
pink	47	2000

FIGURE 5. **SDS-PAGE analysis of Ni-NTA chromatography fractions.** Fractions from Ni-NTA chromatography were run on a 12.5% separating SDS-PAGE gel, along with a BenchMark Pre-Stained Protein Ladder and cell extract from cell lysis (see Table 2 for contents of each lane).

Table 2
Contents of each lane in SDS-PAGE analysis (Fig. 5).

| lane	sample	column volume (mL)	conc. imidazole (mM)
1	ladder	–	–
2	cell extract	–	–
3	flow-through	8	–
4	wash 1	13	25
5	wash 4	28	50
6	wash 5	33	75
7	wash 6	38	100
8	elution 1	39	250
9	elution 2	40	250
10	elution 3	41	250
11	elution 4	42	250
12	elution 5	43	500
13	elution 6	44	500
14	elution 7	45	500
15	elution 8	46	500

DISCUSSION

In this study, we successfully generated a mutant HICA protein, in which the K129 and L133 residues were mutated to histidines. These residues were chosen for mutation because PyMOL analysis confirmed their location on the surface of the HICA protein, their close proximity (between 4.4 to 6.4 Å) to pre-existing histidine residues on the same chain, and an estimated proximity of between 3.7 to 6.7 Å to these same histidines following mutation of K129 and L133 to His (Fig. 1). These distances between histidines were assumed to be favorable for nickel coordination based on previous research that demonstrated that distances of 5 to 7 Å between histidines on the same chain in ECCA were able to bind so strongly to the nickel column that the protein required 250 – 300 mM imidazole to elute (1). Thus, the mutation of the K129 and L133 residues to His was predicted to optimize coordination to nickel, since the newly engineered His residues would be close enough to the pre-existing ones to form a cluster of histidines. As it was previously demonstrated that mutating HICA's Arg160 residue to His sufficiently recreated ECCA's metal affinity (1), we knew that this method of engineering a histidine cluster was effective, however, we wanted to explore whether that cluster could be engineering on other locations on the solvent-exposed surface of HICA. When exploring other areas of the surface of the protein, the K129 and L133 residues were also chosen based on the fact that they were far from the zinc-containing active site. Therefore, mutation of this region would not be predicted to interfere with enzymatic function of the protein.

Although the K129 and L133 mutations were designed to generate a protein with favorable inter-histidine distances for nickel binding, our data suggest that our K129 L133 mutant HICA protein exhibits weak nickel affinity. From the SDS-PAGE results (Fig. 5), it appears that most of the mutant HICA protein elutes with only 25 mM imidazole, since the

protein was only present in appreciable quantities in the cell extract, flow-through, and 25 mM imidazole wash, and was present only negligibly in the washes and elutions of higher imidazole concentration. However, there were no washes performed with concentrations below 25 mM imidazole, so it is possible that the mutant HICA protein would have eluted with even lower concentrations of imidazole. This does not come close to recapitulating the nickel-binding affinity of ECCA, which requires 250 to 300 mM imidazole to elute (1). Our mutant was also much less effective than the Arg160His mutant, which required 190 mM imidazole (1). One hypothesis as to why our K129 L133 mutant HICA protein did not exhibit the strong nickel binding predicted could be that the mutations were not actually made to an area of the protein that was solvent-exposed. Though PyMOL showed the region on the surface of the protein, it could be that the solvent does not actually penetrate into that groove in the protein. Another reason could be that although there were four histidines in the cluster, they were not actually the right distances from each other, or there were not enough of them to bind to the Ni^{2+}.

Since we were unable to perform tests on the kinetic activity of our mutant HICA protein, we do not know if the mutation affected enzymatic activity. However, we can infer from what we know about the HICA mechanism, that our mutation most likely did not affect the enzymatic activity, as the mutation was not made to the zinc-containing active site. The fundamental structural unit of HICA is a dimer composed of two identical protein chains (8). All β-carbonic anhydrases contain one zinc ion per monomer in a pseudo-tetrahedral coordination environment of the type $Cys_2His(X)$, where X is water, an anion or an Asp residue. HICA is a type II β-carbonic anhydrase, meaning that its active site zinc ion is coordinated to 4 protein ligands, Cys42, Asp44, His98, and Cys101. HICA also has a narrow, hydrophobic active site cleft that lies along the dimer interface and leads to the active site zinc ion. This zinc helps to catalyze the reaction:

$$CO_2 + H_2O \rightleftharpoons HCO_3^- + H^+$$
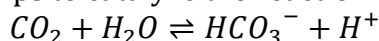
In the forward reaction, CO_2 is concentrated in the active site by association with hydrophobic residues that line that active site cleft. The CO_2 is then positioned for nucleophilic attack by a zinc-bound hydroxide ion, which is oriented by the Asp residue. The zinc-bound hydroxide undergoes a nucleophilic addition to CO_2, converting it to a bicarbonate ion. The developing negative charge on the bicarbonate ion is stabilized by H-bonding to a Gln 151' residue. Then water exchanges for bicarbonate at the zinc ion, and a proton is lost from the zinc-bound water to regenerate the zinc-bound hydroxide ion. Understanding this mechanism allowed us to choose mutation sites (K129 and L133) in the HICA monomer that were located far from the monomer's zinc active site. However, kinetic data still needs to be collected to ensure that enzymatic function was in fact undisrupted.

REFERENCES
1. Hoffman, K. M., Wood, K. M., Labrum, A. D., Lee, D. K., Bolinger, I. M., Konis, M. E., Blount, A. G., Prussia, G. A., Schroll, M. M., and Watson, J. M. (2014) Surface histidine mutations for the metal affinity purification of a β-carbonic anhydrase. *Anal. Biochem.* **458**, 66-68
2. Langereis, J. D., Zomer, A., Stunnenberg, H. G., Burghout, P., and Hermans, P. W. M. (2013) Nontypeable Haemophilus influenzae carbonic anhydrase is important for environmental and intracellular survival. *J. Bacteriol.* **195,** 2737-2746

3. Barik, S. (1996) Site-directed mutagenesis in vitro by megaprimer PCR. *Methods Mol. Biol.* **57**, 203-215.
4. Roux, K. H. and Hecker, K. H. (1997) One-step optimization using touchdown and stepdown PCR. *Methods Mol. Biol.* **67**, 39-45.
5. Smith, P. K., Krohn, R. I., Hermanson, G. T., Mallia, A. K., Gartner, F. H., Provenzano M. D., Fujimoto, E. K., Goeke, N. M., Olson, B. J., and Klenk, D. C. (1985) Measurement of protein using bicinchoninic acid. *Anal. Biochem.* **150**, 76-85.
6. Block, H., Maertens, B., Spriestersbach, A., Brinker, N., Kubicek, J., Fabis, R., Labahn, J., and Schäfer, F. (2009) Immobilized-metal affinity chromatography (IMAC). *Methods Enzymol.* **463**, 439-473.
7. Laemmli, U. K. (1970) Cleavage of structural proteins during assembly of the head of bacteriophage T4. *Nature.* **227**, 680-685.
8. Rowlett, R. S. (2009) Structure and catalytic mechanism of the β-carbonic anhydrases. *Biochim. Biophys. Acta*. **1804**, 362-372.

ACKNOWLEDGEMENTS